Ca and Mg isotope fractionation during the stoichiometric dissolution of dolomite at temperatures from 51 to 126 °C and 5 bars CO_2 pressure

A. Perez-Fernandez[1], U.-N. Berninger[1], V. Mavromatis[1,2], P.A.E. Pogge von Strandmann[3], and E.H. Oelkers[1,3]

[1] Géosciences Environnement Toulouse, CNRS-UPS-OMP, 14, Av. Edouard Belin, 31400 Toulouse, France

[2]Institute of Applied Geosciences, Graz University of Technology, Rechbauerstrasse 12, 8010 Graz, Austria.

[3] London Geochemistry and Isotope Centre (LOGIC), Institute of Earth and Planetary Sciences, UCL and Birkbeck, University of London, Gower Street, London, WC1E 6BT, United Kingdom.

Abstract – Natural polycrystalline hydrothermal Sainte Colombe dolomite was dissolved in stirred titanium closed system reactors in aqueous 0.1 mol/kg NaCl solutions at 51, 75, 121, and 126°C and a pressure of 5 bars CO_2. In total, 52, 27, 16, and 12%, respectively, of the dolomite placed in the reactors dissolved into the fluid phase during these experiments. Each experiment lasted from 12 to 47 days and the fluid phase in each evolved towards, but did not exceed, ordered dolomite equilibrium at a pH of 5.9±0.3. All aqueous reactive fluids were undersaturated with respect to all potential secondary phases including calcite and magnesite. The reactive fluid compositions at the end of the experiments had a molar Ca/Mg ratio equal to that of the dissolving dolomite, and the dolomite recovered after the experiments contained only pure dolomite as verified by scanning electron microscopy. The Ca and Mg isotopic ratios of the reactive fluids remained within uncertainty equal to that of the dissolving dolomite in the experiments performed at 51 and 75 °C. In contrast, the Ca isotopic composition of the reactive fluid in the experiment performed at 121 and 126 °C was significantly greater such that $\Delta^{44/42}Ca_{solid\text{-}fluid}$ = -0.6±0.1‰, whereas that of Mg was within uncertainty equal to that of the dissolving mineral. The equilibrium fractionation factors for both divalent cations favor the incorporation of isotopically light metals into the dolomite structure. Our results at 121 and 126 °C, therefore, are consistent with the one-way transfer of Mg from dolomite to the fluid but the two-way transfer of Ca from and to dolomite as equilibrium is approached during its stoichiometric dissolution. The lack of Mg returning to

the dolomite structure at these conditions is attributed to the slow dehydration kinetics of aqueous Mg. As more than 12% of the dolomite dissolved during the 121 and 126 °C closed system experiments, our observations indicate a significant change in the Ca isotopic signature of the dolomite during its stoichiometric dissolution. Moreover, as there is no visual evidence for dolomite recrystallization during this experiment, it seems likely that the resetting of Ca isotopic signatures of carbonate minerals can be readily overlooked in the interpretation of natural systems.

Keywords: Dolomite precipitation, dissolution, Ca isotopes, Mg, isotopes, mineral growth

1. **Introduction**

Dolomite is widely distributed in Earth's crust, however, its origin has puzzled the scientific community over the last century. This "dolomite problem" stems from its poor distribution in recent marine sediments compared to its common occurrence in ancient sedimentary records (Arvidson and Mackenzie, 1999; Holland, 2005). In an attempt to resolve this problem, numerous authors have studied the kinetic and thermodynamic behavior of this mineral (e.g. Arvidson and Mackenzie, 1999; Busenberg and Plummer, 1982; Chou et al., 1989; Gautelier et al., 1999, 2007; Lund et al., 1973; Morse and Arvidson, 2002; Pokrovsky et al., 1999a, 1999b, 2005, 2009; Putnis et al., 2014; Wollast, 1990; Zhang et al., 2007). It has been observed that Ca is initially released faster to the fluid than Mg during far-from-equilibrium dolomite dissolution (Busenberg and Plummer, 1982; Pokrovsky and Schott, 2001; Pokrovsky et al., 1999a; Putnis et al., 2014); this initial incongruent dissolution was explained by the formation of Mg-rich surface complexes (Pokrovsky and Schott; 1999; Pokrovsky et al. 1999a, b; Van Cappellen et al., 1993). Numerous studies have concluded that the "dolomite problem" is a kinetic issue that stems from ether the slow dehydration of aqueous magnesium at ambient temperatures or the deformation of the crystal structure due to the incorporation magnesium, yet the detailed mechanisms and the conditions at which dolomite may form remain unclear (Arvidson and Mackenzie, 1999; Land, 1980, 1998; Pokrovsky et al., 1999a).

The divalent metal isotope compositions of carbonate minerals have been interpreted to illuminate the temporal evolution of the global calcium cycle (De la Rocha and DePaolo, 2000; Fantle and DePaolo, 2005), global bio-geochemical cycles (DePaolo, 2004; Fantle, 2010; Nielsen et al., 2012), ocean chemical evolution (Gussone et al., 2005; Hauser et al., 2005; Sime et al., 2007), past continental weathering (Beinlich et al., 2014; Galy et al., 2002; Gussone et al., 2003; Fantle and DePaolo, 2005; Immenhauser et al., 2010; Kasemann et al., 2014; Li et al., 2014; Mavromatis et al., 2014b; Pogge von Strandmann et al., 2008, 2012), paleotemperatures (Galy et al., 2002; Gussone et al., 2003; Marriott et al., 2004; Mavromatis et al., 2012, 2013, 2014a), and ancient climatic events (DePaolo, 2004; Kasemann et al., 2014; Pogge von Strandmann et al., 2014). Such potential applications have motivated a number of studies of Mg and Ca isotopic fractionation among carbonate minerals and coexisting aqueous fluids (e.g. Immenhauser et al., 2010; Pearce et al., 2012; Mavromatis et al., 2013, 2014a). Some of these studies report that isotopically lighter Ca is preferentially

incorporated into carbonate minerals as it is precipitated from an aqueous fluid (De la Rocha and DePaolo, 2000; DePaolo, 2004; Gussone et al., 2003, 2005; Skulan et al., 1997; Zhu and Macdougall, 1998). Such observations have been attributed to both equilibrium and kinetic processes (DePaolo, 2011; Gussone et al., 2003, 2011; Lemarchand et al., 2004; Marriott et al., 2004; Reynard et al., 2010, 2011; Tang et al., 2008a, 2008b). Lemarchand et al. (2004) suggested that the equilibrium distribution of Ca isotopes between a fluid and a solid phase can be overprinted by the incorporation of unequilibrated Ca into the crystal structure at elevated precipitation rates. In addition, as light isotopes diffuse faster than their heavier counterparts, lighter isotopes may be preferentially released during dissolution or incorporated into the mineral during precipitation (Gussone et al., 2003; Maher et al., 2016; Richter et al., 2006).

Past studies have shown that Mg isotopes can be fractionated both during precipitation (Immenhauser et al., 2010; Li et al., 2012; 2015; Mavromatis et al., 2012, 2013, 2014a; Shirokova et al. 2013; Wombacher et al., 2011, Young and Galy, 2004) and dissolution (Pearce et al., 2012) of carbonate minerals. Generally, carbonate minerals are enriched in lighter Mg, as is the case for Ca. This behavior stems from the relative strength of the Mg-O bond in the carbonates compared to the aqueous solution (Mavromatis et al., 2013; Schott et al., 2016). Higgins and Schrag (2010) and Mavromatis et al. (2014a) suggested an ambient temperature fluid-dolomite equilibrium fractionation factor ($\Delta^{26/24}Mg_{solid\text{-}fluid} = \delta^{26/24}Mg_{solid} - \delta^{26/24}Mg_{fluid}$) of ~-2.6‰ from field observations, whereas Schauble (2011) suggested this fractionation factor should be -3.6‰ from ab-initio calculations. Direct experimental measurements indicate these fractionations factors decrease with increasing temperature such that $\Delta^{26/24}Mg_{solid\text{-}fluid}$ = -0.93% at 130 ^{o}C (Li et al., 2015). Li et al. (2015) and Pinilla et al. (2015) concluded that that disordered dolomite and Mg-calcite have lower fractionation factors than ordered dolomite due to the distortion of the cationic sites that originate longer Mg-O bond lengths. The fractionation of Mg between carbonate minerals and the fluid phase can also be affected by other factors like 1) kinetic processes such as the carbonate mineral growth rate (Mavromatis et al., 2013), 2) the Mg speciation of the fluid (Schott et al., 2016), and 3) biologically mediated vital effects (Hippler et al., 2009; Pogge von Strandmann et al., 2008, 2014; Rollion-Bard et al., 2016). Although some results published in the literature suggest that fluid-carbonate mineral Mg isotope fractionation is relatively independent of reactive solution pH (Mavromatis et al., 2013) and the fraction of dissolved organic molecules

(Ilina et al., 2013), the theoretical and experimental modeling of Schott et al. (2016), suggests that changes in the aqueous complexation of Mg can alter dramatically this fractionation.

As dolomite contains equal molar quantities of Ca and Mg, and these occupy analogous positions in the crystal structure, this mineral has the potential to illuminate the isotopic fractionation behavior of both metals. The quantification of dolomite isotopic systematics during its interaction with fluids, however, is limited by its inability to precipitate at ambient temperatures in the laboratory (Li et al., 2015). To overcome these limitations numerous studies have been aimed at characterizing the Ca and Mg isotope systematics of natural dolomites (Blättler et al., 2015; Fantle and Higgins, 2014; Geske et al., 2015; Holmden, 2009; Jacobson et al., 2010; Mavromatis et al., 2014a; Pokrovsky et al., 2011; Rustad et al., 2010; Schauble, 2011). It has been suggested that because of their similar chemistry, Ca isotope fractionation in carbonate minerals should be similar to that of Mg (Pearce et al., 2012). Alternatively, contrasting fractionation behaviors of Ca and Mg isotopes was reported as a function of depth in authigenic dolomites by Blättler et al. (2015). These observations, however, were interpreted to be a consequence of a limited Mg supply in the pore water.

This study was designed to advance our understanding of the behavior of Mg and Ca isotopes during dolomite-water interaction. Towards this goal, pure dolomite was dissolved stoichiometrically in closed system reactors at 51, 75, 121, and 126 °C. The purpose of this manuscript is to report the chemical and isotopic evolution of the fluids and solids in these experiments and to use the results to better understand the reactivity of dolomite in natural systems.

2. Theoretical considerations:

Isotope compositions in this paper are presented in delta notation given by (McKinney et al., 1950; Urey, 1948)

$$\delta\,{}^{A}M = \left(\frac{{}^{A}M_{sample}}{{}^{A}\mathrm{M}_{tandard}} - 1\right)1000 \qquad (1)$$

where ${}^{A}M$ refers to the *A*th isotope ratio of the *M*th metal (e.g. $^{44}Ca/^{42}Ca$ or $^{26}Mg/^{24}Mg$), $\delta^{A}M$ provides the normalized value of this ratio, and the subscripts *sample* and *standard* represent the sample of interest and an isotopic standard, respectively. Mg results are reported with respect to the DSM3 international standard and Ca results with respect to the NIST SRM915a standard.

The isotopic offset between the metal in the solid and the fluid phase ($\Delta^{A}M_{solid-fluid}$) is defined by

$$\Delta^{A}M_{solid-fluid} = \delta^{A}M_{solid} - \delta^{A}M_{fluid} \quad (2)$$

Note that as it was not possible to directly measure the degree of isotopic heterogeneity of the solids during our experiments, the average isotopic composition of the solids was used in this calculation. The average isotopic composition of the solid phase during a closed system stoichiometric dissolution experiment can be calculated from that of the fluid phase from mass balance considerations by taking account of (Criss, 1999)

$$\delta^{A}M_{total}m_{M,total} = \delta^{A}M_{solid}m_{M,solid} + \delta^{A}M_{fluid}m_{M,fluid} \quad (3)$$

where $m_{M,soilid}$ and $m_{M,fluid}$ refer to the mass of the metal *M* in the solid and fluid phase, respectively, and noting that the product $\delta^{A}M_{total}m_{M,total}$ is constant in a closed system reactor.

Within the context of transition state theory, mineral dissolution consists of two coupled processes, the removal of material from the mineral surface, sometimes referred to as forward dissolution, and the inverse process, sometimes referred to as returning some of the dissolved material back to this surface. This latter inverse reaction, sometimes referred to as reverse precipitation, is negligible in strongly undersaturated fluids but becomes increasingly important as the fluid composition approaches equilibrium (Aagaard and Helgeson, 1982; Oelkers, 2001; Schott and Oelkers, 1995; Schott et al., 2009, 2012). At equilibrium the reverse reaction is equal in rate to forward dissolution, such that the net rate is zero. This concept that the reaction does not stop at equilibrium, but the net reaction rate is zero due to the forward and reverse reaction being equal but opposite, is commonly termed 'dynamic equilibrium'. It is unclear, however, if this inverse reaction occurs in all mineral-fluid systems, as numerous minerals do not precipitate at ambient conditions. For example, whereas

anhydrous calcium carbonate minerals such as calcite and aragonite can readily precipitate abiotically at ambient temperatures, anhydrous magnesium carbonate minerals, such as magnesite and ordered dolomite are found not to precipitate abiotically at such conditions (Baker and Kastner, 1981; Berninger et al., 2016, 2017; Gautier et al., 2015, 2016; Katz and Matthews, 1977; Land, 1998; Liberman, 1967; Saldi et al., 2012; Sibley et al., 1987). This contrasting behavior has commonly been attributed to the vastly different hydration of aqueous calcium compared to aqueous magnesium, such that the more strongly hydrated Mg limits its ability to be incorporated into the dolomite surface from aqueous solutions (e.g. Deelman, 2001; De Leeuw and Parker, 2001; Haamm et al., 2010; Higgins and Hu, 2005; Lippmann, 1973; Yang et al., 2012).

In the absence of the reverse reaction, isotopic fractionation during the stoichiometric dissolution of a mineral would require the preferential release of distinct isotopologues from the mineral to the fluid. For an initially isotopically homogeneous mineral, this would require isotope fractionation during solid-state diffusion towards the mineral surface. In contrast, if reverse reactions can occur in the system, isotope fractionation during the stoichiometric dissolution of a mineral could proceed by the conservative release of isotopologues during the forward dissolution step coupled to a preferred reincorporation of distinct isotopologues during the reverse reaction step. As calcium and magnesium exhibit distinct precipitation behaviors in carbonate minerals at ambient temperatures (e.g. anhydrous calcium carbonate readily precipitates whereas anhydrous magnesium carbonates are kinetically inhibited) it might be expected that their isotopic fraction may also exhibit distinct behaviors.

3. Materials and methods

3.1 Experimental procedure

Natural polycrystalline hydrothermal Sainte Colombe dolomite (Gautelier et al., 1999) was hand crushed with agate mortar and pestle, sieved to 100-150 mesh, magnetically separated to remove iron-bearing particles and handpicked under an optical microscope. The resulting dolomite powder was reacted for a few seconds in $0.1N\ HCl$, rinsed with deionized water, ultrasonically cleaned using ethanol and dried at 60° for 24 h. A Scanning Electron Microscope (SEM) image, obtained using a JEOL JSM-6360 LV microscope of the resulting cleaned dolomite is shown in Fig. 1a. The image shows the powder to consist of only

dolomite and to be free of adhering fine particles. The specific surface area of the prepared dolomite was determined to be 0.717±0.07 m^2/g by multipoint nitrogen adsorption according to the BET method (Brunauer et al., 1938) using a Quantachrome Gas Sorption system. The chemical composition of the dolomite seed material was determined by electron microprobe analysis using a Cameca SX50 and is reported in Table 1**.** The purity of this dolomite was verified via X-ray diffraction (XRD) using an INEL CPS-120 diffractometer with Co Kα-radiation, λ=1.78897 Å and a graphite monochromator. Scans were performed from 1 to 110º 2θ at 0.09º/min and a step size of 0.029º. This analysis demonstrates that the solid is pure dolomite; superstructure reflections (e.g. Lippmann, 1973) indicate the cation-ordered structure of this dolomite.

Four dolomite dissolution experiments were performed in closed-system titanium autoclaves similar to those described by Bénézeth et al. (2011) and Pearce et al. (2012). Approximately 440ml of an aqueous $0.1N\ NaCl$ solution, prepared using high purity (18.2MΩ) water was placed into a reactor; one gram of dolomite powder was then added to this solution. The reactors were closed and placed in a temperature-controlled furnace. The temperature was increased to 51, 75, 121 or 126 °C and it was kept constant over the duration of the experiments which lasted 47, 28, 35, and 12 days respectively. Pure CO_2(g) (<99.99% CO_2) was introduced into the reactor maintaining a constant pressure of 5 bars throughout all of the experiments. The mineral-fluid mixture was continuously stirred at 200rpm. Initial experimental conditions are listed in Table 2. The fluid phase was sampled regularly using a sampling tube comprised of a 2µ titanium filter and a cooling system. A total of 5ml of fluid was collected during each sampling, and these fluids were stored in 10ml polycarbonate containers prior to analysis. The pH was measured immediately after sampling with a standard glass Mettler Toledo pH electrode calibrated with NBS buffers (pH=4.006, 6.865 and 9.183 at 25°C), regression line corrections were applied to adapt measurements to ambient temperature. The fluids and solids remaining in the reactor at the end of the experiments were recovered and filtered through a Teflon 0.45µ filter. The recovered solids were ultrasonically cleaned in ethanol and dried at 60°C during 24h.

The Ca and Mg concentration of the sampled fluids were measured by flame Atomic Absorption Spectroscopy (AAS) using a Perking Elmer AAnalyst 400 with an uncertainty of $\pm$1% and a detection limit of 7 x 10^{-7} mol/kg for Ca and 2 x 10^{-7} mol/kg for Mg. Alkalinity

was determined with an automatic Schott TitroLine alpha TA10plus titrator with an uncertainty of ± 2% and a detection limit of 5×10^{-7} eq/kg. Measured fluid compositions were interpreted using PHREEQC (Parkhurst and Appelo, 1999) together with its PHREEQC database and solubility products reported for the dolomite hydrolysis reaction reported by Berninger (2016) ($\log_{10} Ksp_{(Dol)}$ equals 17.6, 18.6, 20.3 and 20.4 at 51, 75, 121 and 126 °C, respectively).

3.2 Calcium isotope analysis

Calcium was purified using double column ion exchange chromatography following the method described by Reynard et al. (2010) and Blättler et al. (2011). Fluid samples were evaporated to dryness, re-dissolved in concentrated HNO_3, re-evaporated to dryness, then dissolved in $2N\ HCl$ prior to loading onto columns. For the analysis of solids, 0.1mg of the selected solid was first dissolved in concentrated HNO_3, evaporated to dryness and then dissolved again in $HCl\ 2N$. Aliquots of the resulting fluids were loaded into 10ml Bio-Rad poly-propylene columns containing a 200-400mesh AG-50W-X12 resin. The fraction recovered from the columns was evaporated to dryness and dissolved in $3N\ HNO_3$. The yields of this cation exchange step were evaluated by collecting an elute split before and after the main collection bracket for each sample, and checking those splits for Ca content. This showed that column yields were >99.5% for Ca. A second pass through 2ml columns containing Eichrom Sr-spec resin 50-100mesh was used to quantitatively remove Sr, thus avoiding interference during isotopic measurements; fluid samples collected from the first pass of the columns were loaded onto 2ml in-house made PFA columns containing Eichrom Sr-spec resin 50-100mesh. The samples collected following their passing through the second column were evaporated to dryness and redissolved in 2% HNO_3 ready to measure in the MC-ICPMS.

Calcium isotope ratios were determined by sample-standard bracketing using a Nu Instruments Multi Collector Inductively Coupled Plasma Mass Spectrometers (MC-ICP-MS), fitted with a DSN desolvation nebulizer, located in the Earth Sciences Department of Oxford University (UK) as described by Halicz et al. (1999), Reynard et al. (2001) and Blättler et al. (2011, 2015). Due to isobaric interferences with the Ar plasma, precise measurements of ^{40}Ca are not possible, but ^{42}Ca, ^{43}Ca, and ^{44}Ca have abundances of 0.65%, 0.13% and 2.1%, respectively and are convenient for high precision measurements (Halicz et al., 1999). Any

potential hydrides could not be directly resolved, but were assessed, for example, at mass 45 by determining a CaH/Ca ratio. Hydride formation was found to be insignificant, although a corrections were applied to other Ca masses. Moreover, our method of intensity-matching within 5% between samples and bracketing standards also corrects for potential hydride formation. Accuracy and precision were assessed by repeated analyses of the JDol-1 dolomitic standard ($\delta^{44/42}$Ca = 0.46 ± 0.04‰ (2sd), compared to 0.52±0.18‰ of Wombacher et al., 2009) and the IAPSO seawater ($\delta^{44/42}$Ca = 1.06 ± 0.10‰ (2sd), within uncertainty of that measured by Hippler et al., 2003 of 0.94 ± 0.07‰) standards, in keeping with the long-term analytical reproducibility over a period of three years of ±0.16‰ on $\delta^{44/42}$Ca; negligible variations within uncertainty after three passes throughout the whole process were observed (See Table A1 in the Appendix). Results obtained for these standards are within analytical uncertainty of other studies (e.g. Hippler et al., 2003; Reynard et al., 2011). Potential isobaric Sr interferences were corrected by monitoring mass 43.5. While an on-line correction for Sr was applied (using Sr isotope ratios measured each analysis day using a Sr standard), due to the quantitative Sr removal during chemistry, this correction never accounted for more than a 0.005‰ change (Reynard et al., 2011). An in-house standard ("HPSCa", $\delta^{44/42}$Ca = 0.34‰ relative to SRM-915a) was analysed between each sample bracket (Blättler et al., 2011). The total procedural blank was <8 ng, insignificant compared to the ~10μg of Ca aspirated during each analysis. Analyses are reported relative to the Ca isotope standard NIST SRM-915a.

3.3 Magnesium isotope analysis

Selected fluid samples were analysed to determine their Mg isotopic compositions following the method described in Pearce et al. (2012) and Mavromatis et al. (2013, 2014a,b). Typically, 5–10 μg of Mg was processed for each fluid sample, and ~10 mg of dolomite was dissolved in concentrated aqueous HCl, for the solid. Each sample was evaporated until dry then dissolved in concentrated aqueous HNO_3 prior to analysis. The samples were then passed through AG50W-X12 cation exchange resin before being isotopically analysed using a Thermo-Finnigan 'Neptune' MC-ICP-MS at the Géosciences Environnement Toulouse. Samples were introduced into the Ar Plasma via 2% aqueous HNO_3 using a standard sample induction system (SIS), attached to a PFA Teflon nebuliser. Instrumental mass fractionation effects were corrected via sample-standard bracketing using the DSM3 standard (Galy et al., 2003), with total procedural blanks having a negligible contribution; total procedural blank

was <10 ng, which insignificant compared to the ~10μg of Mg analyzed. All sample analyses were run in triplicate. The long-term reproducibility of $\delta^{26/24}$Mg was assessed by multiple measurements of the DSM3 Mg standard. These measurements yielded standard deviations (2σ) of less than 0.09‰. The reproducibility of $\delta^{26/24}$Mg measurements for the liquid Mg standards DSM3, CAM1, and OUMg and the dolomite carbonate standard JDo-1 used during this study was better than 0.03‰, 0.05‰, 0.08‰ and 0.02‰ (2σ), respectively (Table 3).

4. Results

The chemical evolution of the reactive fluid is listed in Table 3 and illustrated in Fig 2a. For all experiments the reactive fluid Ca and Mg concentration increased continuously, approaching a constant value after ~37, 17, 1, and 1 days, respectively, for the experiments at 51, 75, 121 and 126 °C. Calcium was preferentially released relative to Mg at the beginning of each experiment, with measured molar Ca/Mg ratios of as much as 1.2, 1.16, 1.75 and 2.26 during the first few minutes of the experimental run at 51, 75, 121 and 126 °C. Note however, the some of the early analysis of the 121 °C experiment exhibits some analytical scatter. Subsequent metal release from the dolomite was stoichiometric such that fluid samples collected after one day had an atomic Ca/Mg ratio equal to 1 ±0.1. The final Ca and Mg concentrations of the fluids are $6.6x10^{-3}$, $3.4x10^{-3}$, $2.1x10^{-3}$ and $1.8x10^{-3}$ for the 51, 75, 121 and 126 °C experiments; mass balance calculations taking into account these final fluid compositions indicate that 51, 27, 17 and 12% of the original dolomite dissolved during the 51, 75, 121 and 126 °C experiments. Note that dolomite has a retrograde solubility such that the final near to equilibrium cation concentrations and alkalinity decrease with increasing experimental temperature. The fluid pH in each experiment increased rapidly during the first day attaining a value of 6.1±0.05, 5.9±0.06, 5.7±0.04 and 5.6±0.05 at 51, 75, 121 and 126 °C. The saturation index of the reactive fluids with respect to dolomite increases systematically towards, but does not pass zero, consistent with the approach of these experimental systems to equilibrium (see Fig 2c).

Representative photomicrographs of dolomite collected after the experiments are shown in Fig. 1 b to d. SEM analysis revealed only the presence of pure dolomite in the post experiment samples. Dolomite grains after the experiments show clear dissolution features including grain rounding and etch pit formation. These features are most evident in the samples collected from the 51 °C experiment, which exhibited the largest amount of

dissolution. The purity of the dolomite is also confirmed by the atomic Ca/Mg ratios of the reactive fluids, which match closely that of the dissolving dolomite.

The temporal evolution of the reactive fluid $\delta^{26/24}$Mg and $\delta^{44/42}$Ca during all experiments is illustrated in Fig. 3 and reported in Table 3; a complete list of all measured Mg and Ca isotopic compositions including $\delta^{43/42}$Ca and $\delta^{25/24}$Mg are listed in Table A2 of the Appendix. All but two of the measured $\delta^{43/42}$Ca and $\delta^{25/24}$Mg are consistent within uncertainty of that calculated using the corresponding $\delta^{26/24}$Mg and $\delta^{44/42}$Ca values and the assumption of mass dependent fractionation. The reactive fluid isotopic compositions of Ca and Mg are equal within uncertainty of those of the dissolving dolomite in the 51 and 75 °C experiments, consistent with the conservative release of their isotopologues. In contrast, the reactive fluid isotopic Ca compositions are significantly different from that of the dissolving dolomite in the 121 and 126 °C experiments. The reactive fluid Ca compositions in these experiments ($\delta^{44/42}$Ca) are as much as 0.67‰ higher than that of the dissolving dolomite, whereas the reactive fluid Mg ($\delta^{26/24}$Mg) is as much as 0.19‰ lower than that of the original solid.

5. Discussion

5.1 Dolomite dissolution behavior

Calcium was observed to be preferentially released compared to Mg over the first few minutes of each closed system dolomite dissolution experiment (see Table 3 and Fig A1). This observation is consistent with previous reported by Busenberg and Plummer (1982) and the suggestion that the dolomite-water interface is dominated by the presence of Mg-rich surface complexes (Pokrovsky and Schott, 1999; Pokrovsky et al., 1999a, 1999b; Van Cappellen et al., 1993). Dolomite dissolution continued to proceed by the stoichiometric release of Ca versus Mg consistent with its congruent dissolution (see Fig. A1 in the appendix). Note that in these batch experiments, the Ca/Mg ratio of the fluid phase reflects the cumulative release of these metals over the whole of the experiment. The congruent dissolution of dolomite is confirmed by geochemical fluid speciation calculations that indicate that the reactions fluids are undersaturated with respect to all minerals in the PHREEQC database, including dolomite itself. Dolomite dissolution rates were not retrieved from the closed system experiments in this study because 1) the pH of the fluids were allowed to drift – from ~ 4 to 6 during each experiment, and 2) the experiments were designed to dissolve a large fraction of the original dolomite. As much as 50% of the original dolomite dissolved

during these experiments so that the dolomite-water interfacial surface area evolved substantially. As dolomite dissolution rates are functions of both reactive fluid pH and surface area (Busenberg and Plummer, 1982; Gautelier et al., 1999, 2007; Pokrovsky et al., 2005; Pokrovsky and Schott, 2001), dolomite dissolution rates likely varied continuously throughout these experiments making the potential retrieval of dissolution rates from these experiments ambiguous.

5.2 Calcium and magnesium isotope behavior during dolomite dissolution

The results presented above indicate that the Ca and Mg isotopic compositions of the reactive fluids in the experiments performed at 50 and 75 °C are equal within uncertainty to that of the dissolving dolomite. These observations contrast greatly with that observed during the >100 °C experiments. In the higher temperature experiments, the reactive fluid Ca composition ($\delta^{44/42}$Ca) is ~0.6‰ heavier and the Mg is initially somewhat lighter than the dissolving dolomite. There is also a slight trend for the fluid phase to become isotopically heavier in Mg as the experiments progress as evident in Fig. 3.

Insight into the origin of these differences can be made through the aid of transition state theory. The overall dissolution process consists of two coupled reactions: forward dissolution, which is the removal from material from the mineral to the fluid phase, and reverse precipitation, which is the tendency for some of the material to return and to be reincorporated into the mineral structure. In the absence of substantial solid-state diffusion or isotope heterogeneity in the mineral, the forward dissolution process would not lead to substantial non-conservative isotopic release of metals. In contrast, the reverse precipitation step could, if it occurred lead to isotope fractionation as is commonly observed in mineral precipitation experiments (e.g. Li et al., 2012;Macromatis et al., 2012; Saulnier et al., 2012) .

We hypothesize, therefore, that the origin of the contrasting isotopic release of divalent metals from dolomite at temperatures below 100°C compared to that at higher temperatures stems from a change in dolomite reactivity. At < 100°C, the isotopic composition of Ca and Mg is the fluid phase is identical to that of the dissolving dolomite. This observation is

consistent with the one-way transfer of these metals from the mineral to the fluid phase in the absence of reverse precipitation. A large number of studies have observed that dolomite does not precipitate at temperatures below 100 °C (Arvidson and Mackenzie, 1999; Higgins and Hu, 2005; Land, 1998; Li et al., 2015; Vasconcelos et al., 2005). Abiotic laboratory synthesis of ordered dolomite generally requires hydrothermal conditions (Kessels et al., 2000). Indeed, Rodriguez-Blanco et al. (2015) observed that abiotic ordered dolomite precipitation occurred only at temperatures in excess of 140 °C. Li et al. (2015) succeeded to precipitate disordered, but not ordered, dolomite at 130 °C in the presence of both 1.0 mol/kg $MgCl_2$ and 1.0 mol/kg $CaCl_2$ in the reactive fluid; these authors noted that at such high ionic strengths Mg was not fully hydrated in the reactive aqueous phase. Equally Berninger (2016) noted that it was possible to reverse dolomite aqueous solubility experiments at temperatures ≥ 150 °C, but not possible at ≤ 100 °C.

In contrast to the behavior observed at temperatures < 100 °C, the Ca in the fluid phase at the end of the 121 and 126 °C experiments ($\delta^{44/42}$Ca) was ~0.6‰ heavier than that of the original dolomite. The observed non-conservative release of divalent metal isotopes from the solid is unlikely to be due to heterogeneities in the original dolomite because 1) the dolomite used in experiment was ground from large grains, which tends to homogenize the surfaces even if the original dolomite was isotopically heterogeneous, and 2) the release of Ca and Mg from the 50 and 75 °C experiments was isotopically conservative during the dissolution of as much as 50% of the original dolomite. We interpret the observation that the reactive fluid $\delta^{44/42}$Ca was heavier than that of the dissolving dolomite to be due to the isotopically conservative release of Ca from the dolomite coupled to the return of isotopically light Ca to the dolomite during the reverse precipitation reaction. The tendency of Ca to be lighter in carbonate minerals than the fluid phase from which it precipitated has been commonly reported in the literature (DePaolo, 2011; Gussone et al., 2003, 2011; Lemarchand et al., 2004; Marriott et al., 2004; Reynard et al., 2010, 2011; Tang et al., 2008a, 2008b). Such observations have been attributed to kinetic fractionation effects (Gussone et al., 2003), equilibrium fractionation (Bullen et al., 2003; Marriott et al., 2004), or a combination of equilibrium fractionation affected by coprecipitation processes (Lemarchand et al., 2004; Zhang et al., 2007; Reynard et al., 2011).

In contrast to Ca, however, the isotopic composition of Mg in the fluid phase is close to that of the dissolving dolomite during the 121 and 126 °C experiments. This lack of fractionation during stoichiometric dolomite dissolution suggests that the reverse precipitation reaction is negligible or sluggish at these conditions as a number of studies have reported the that Mg isotopes fractionate substantially in response to dolomite dissolution.. Notably, Li et al. (2015) concluded that at equilibrium ordered dolomite ($\delta^{22/24}$Mg) is 0.93‰ lighter than its co-existing fluid phase at 130 °C. Such observations suggest that if the substantial reverse precipitation of Mg occurred during our experiments we would observe a fluid phase enriched in heavy Mg. We suggest, therefore, that the contrasting behavior between Mg and Ca observed in our 121 and 126 °C experiments stems from their distinct reactivity; the relatively slow incorporation of Mg into the dolomite structure is evidenced by its close to isotopically conservative transfer during our dissolution experiments. Note however, the fluid phase Mg composition is trending slightly heavier over time. This trend may be indicative of the sluggish incorporation rates of Mg into the dolomite structure during our experiments.

Note that as 17 and 12% of the dolomite dissolved during the 121 and 126 °C experiments, mass balance requires that the average Ca isotopic composition of the dolomite present in the rector also evolved during these experiment. Taking account of this mass of dissolved dolomite and the fluid composition of the dolomite at the end of these experiments (see eqn. 3), mass balance requires that the average Ca isotopic composition decreased by 0.12‰ and by 0.10‰ respectively in these experiments. If one compares the final fluid and average dolomite isotopic Ca composition ($\delta^{44/42}$Ca), a final difference of ~0.7‰ is obtained. This difference, however, may not correspond to an equilibrium fractionation factor. The mass transfer to and from the interior of the dolomite grains may be limited by transport processes such that a Ca isotopic gradient develops near the dolomite surface. Due to this potential isotopic gradient, it was not possible to determine the Ca isotope composition of the dolomite surface and thus not possible to determine unambiguously the dolomite-fluid equilibrium fractionation factor for this element from our experiments.

5.3 Insights into dolomite reactivity

The results summarized above suggest that the reverse precipitation is negligible during the dissolution of dolomite at temperatures < 100 °C. The lack of abiotic low-temperature (< 100 °C) dolomite formation has been attributed to both 1) the deformation of the dolomite structure by the incorporation of Mg (Xu et al. 2013; Hong et al., 2016), and 2) a kinetic limitation due to the slow dehydration rates of the aqueous Mg^{2+} cation (Brady et al., 1996; Higgins and Hu, 2005; Lippmann, 1973; Leiberman, 1967; Roberts et al., 2013; Slaughter and Hill, 1991; Wang et al., 2016). There is strong supporting evidence for both of these factors playing a role. The role of Mg deformation in dolomite growth inhibition is supported by the observations of Xu et al. (2013) who failed to precipitate dolomite in the absence of water at ambient temperatures. Stress calculations also show that the incorporation of more than 40% of Mg into the calcite structure leads to plastic deformation, suggesting that the lattice stress mismatch between $MgCO_3$ and $CaCO_3$ inhibits dolomite growth at ambient temperatures (Hong et al., 2016). The role of structural deformation on dolomite growth is also evidenced by atomic force microscopic studies, which have shown that at both ambient temperatures and at temperatures up to at least 120 ^oC dolomite growth is slowed, then completely arrested after the incorporation of one to four layers of Mg onto the dolomite surface (Berninger et al., 2017; Higgins and Hu, 2005). Further support for the importance for structural deformation in dolomite growth inhibition stems from the relative ease in growing dolomite analogues norsethite ($BaMg(CO_3)_2$) and $PbMg(CO_3)_2$ (Linder et al., 2017; Pimentel and Pina, 2014, 2016).

In contrast the role of sluggish Mg dehydration kinetics on dolomite growth kinetics is evidenced by the inhibition of magnesite precipitation from aqueous at temperatures less than 80 ^oC (Saldi et al., 2009, 2012); indeed structural deformation is unlikely to play a role in the incorporation of Mg into this mineral. This behavior contrasts with the observation that hydrated Mg-carbonate phases readily form at ambient conditions (e.g. Berninger et al., 2014; Gautier et al., 2014). As noted by Yang et al. (2012) the structure and dynamics of Mg^{2+} and Ca^{2+} hydration are significantly different; the rate of water exchange around Ca^{2+} is five orders of magnitude faster than that of Mg^{2+}. An associative mechanism for making Ca-CO_3 bonds in the aqueous environment is possible at ambient temperatures, but not viable for making Mg-CO_3 bonds (Di Tommaso and de Leeuw, 2008; Ikeda et al., 2007). A number of studies have argued that the ability of Mg^{2+} desolvating anions or organic compounds to promote Mg-rich calcite and disordered dolomite growth supports the major role of sluggish

Mg dehydration kinetics in inhibiting dolomite growth (e.g. Rodgers, 2013; Zhang et al., 2010).

The results of this study add further support for the role of sluggish aqueous Mg dehydration kinetics on slowing or inhibiting dolomite growth. The temporal variation of the reactive fluid Ca and Mg isotope compositions temperatures of 121 and 126 ^{o}C, suggests that whereas Ca can readily move into and out of the dolomite structure at near to equilibrium conditions at these temperatures. In contrast, evidence presented in this study shows that Mg at best re-enters the dolomite structure relatively slowly at these conditions. These results suggests that aqueous Mg is far slower to enter the dolomite structure than aqueous Ca, which is consistent with calculations reported by Yang et al. (2012) for lower temperature systems. Such evidence, coupled with the large body of evidence summarized above, indicates that both the structural deformation of the dolomite structure and the sluggish Mg dehydration kinetics play a role in inhibiting dolomite formation at temperatures to at least 126 ^{o}C.

Another noteworthy observation is that the during the 121 and 126 ^{o}C more than 10% of the dolomite dissolved into the fluid phase and the fluid phase is $\delta^{44/42}$Ca is ~0.6‰ heavier than the dissolving mineral, yet the fluid Ca:Mg ratio is identical to that of the dissolving dolomite. In the absence of substantial Mg returning to the surface, these observations suggest that the Ca present in the fluid exchanges with the Ca in the dolomite structure in the absence of a similar Mg exchange. Such observations are consistent with numerous past studies which have observed the exchange of one or more elements deep within the solids during congruent mineral or glass dissolution experiments (c.f. Casey et al., 1989; Chou and Wollast, 1989; Oelkers et al., 2009; Schott et al., 2012).

6. Conclusions

The results presented above illustrate the non-conservative transfer of Ca isotopologues during the stoichiometric dissolution of dolomite at 121 and 126 °C. The contrast in this behavior compared to the conservative transfer at lower temperatures is interpreted to stem from the existence of a reverse reaction at higher temperatures. A similar approach was used by Liu et al. (2016) to verify the existence of a reverse reaction for quartz dissolution and to validate the law of detailed balancing. In contrast, Mg is close to conservatively transferred to the fluid phase at these conditions. This latter observation suggests that the departure of Mg into the fluid phase during the dissolution of dolomite at temperatures to at least 126 °C is not

coupled to a rapid reverse reaction reincorporating Mg into the dolomite structure at near to equilibrium conditions. Taken together, these results suggest that it is the inability of Mg to be incorporated into the dolomite structure is a contributing factor limiting the precipitation of this mineral from supersaturated aqueous solutions at low to moderate temperatures.

The observation that dolomite releases Ca non-conservatively during dolomite dissolution at elevated temperature at near to equilibrium is further evidence that mineral isotopic compositions can be altered in the absence of net mineral precipitation. Such a process may question the preservation of isotopic signatures in some systems. Such processes will be explored in further detail in subsequent studies.

Acknowledgements

We would like to thank Aridane Gonzalez, Christian Grimm, Alan Hsieh, Don Porcelli and Thomas Rinder, for helpful discussions over the course of this study. Alain Castillo, Carole Causserand, Thierry Aigouy, Jérôme Chmeleff for their help with analysis. This work was supported by the Centre National de la Recherche Scientifique (CNRS), the Earth Sciences Department of the University of Oxford and the European Commission (through Marie Curie ITN Mettrans Project).

REFERENCES

Aagaard, P., Helgeson, H.C., 1982. Thermodynamic and kinetic constraints on reaction rates among minerals and aqueous solutions; I, Theoretical considerations. American Journal of Science, 282(3): 237-285.

Arvidson, R.S., Mackenzie, F.T., 1999. The dolomite problem; control of precipitation kinetics by temperature and saturation state. American Journal of Science, 299(4): 257-288.

Baker, P.A., Kastner, M. 1981. Constraints on the formation of sedimentary dolomite. Science, 213:214-216.

Beinlich, A., Mavromatis, V., Austrheim, H., Oelkers, E. H., 2014. Inter-mineral Mg isotope fractionation during hydrothermal ultramafic rock alteration – Implications for the global Mg-cycle. Earth and Planetary Science Letters, 392: 166-176.

Berninger, U-N. (2016) On the reactivity of Mg-carbonates. Ph.D.-thesis at Université Toulouse 3 Paul Sabatier and Ludwig-Maximilians-Universität München, 172 pp.

Berninger, U.-N., Jordan, G., Schott, J., Oelkers, E.H., 2017.The experimental determination of hydromagnesite precipitation rates at 22.5-75 ºC. Mineralogical Magazine: 78: 1405-1416.

Berninger, U.-N., Saldi, G.D., Jordan, G., Schott, J., Oelkers, E.H., 2017. Assessing dolomite surface reactivity at temperatures from 40 to 120 ºC by hydrothermal atomic force microscopy. Geochimica et Cosmochimica Acta, 199: 195-209.

Berninger, U.-N., Jordan, G., Lindner, M., Reul, A., Schott, J., Oelkers, E.H., 2016. On the effect of aqueous Ca on magnesite growth – Insight into trace element inhibition of carbonate mineral precipitation. Geochimica et Cosmochimica Acta, 178: 195-209.

Blättler, C. L., Jenkyns, H. C., Reynard, L. M., Henderson, G. M., 2011. Significant increases in global weathering during Oceanic Anoxic Events 1a and 2 indicated by calcium isotopes. Earth and Planetary Science Letters, 309(1–2): 77-88.

Blättler, C.L., Miller, N.R., Higgins, J.A., 2015. Mg and Ca isotope signatures of authigenic dolomite in siliceous deep-sea sediments. Earth and Planetary Science Letters, 419: 32-42.

Brady, P.V., Krumhans, J.L., PApenguth, H.W., 1996. Surface complexation clues to dolomite growth. Geochimica et Cosmochimica Acta, 609, 727-731.

Brunauer, S., Emmett, P.H., Teller, E., 1938. Adsorption of gases in multimolecular layers. Journal of the American Chemical society, 60(2): 309-319.

Bullen, T.D., Kim, S.T., Paytan, A., 2003. Ca isotope fractionation during Ca-carbonate precipitation: There's more to it than temperature. Geochimica et Cosmochimica Acta, 67: A049.

Busenberg, E., Plummer, L.N., 1982. The kinetics of dissolution of dolomite in CO_2-H_2O systems at 1.5 to 65 ^oC and 0 to 1 atm PCO_2. American Journal of Science, 282(1): 45-78.

Bénézeth, P., Saldi, G.D., Dandurand, J.-L., Schott, J., 2011. Experimental determination of the solubility product of magnesite at 50 to 200 °C. Chemical Geology, 286(1–2): 21-31.

Casey, W.H., Westrich, H.R., Arnold, G.W., Banfield, J.F., 1989. The surface chemistry of dissolving laboradorite feldspar. Geochimica et Cosmochimica Acta, 53, 821-832.

Chou, L., Garrels, R.M., Wollast, R., 1989. Comparative study of the kinetics and mechanisms of dissolution of carbonate minerals. Chemical Geology, 78(3): 269-282.

Chou L., Wollast, R.,1989. Is the exchange reaction of alkali feldspars reversible? Geochimica et Cosmochimica Acta 53, 557-558.

Criss, R.E., 1999. Principles of stable isotope distribution. Oxford University Press.

Deelman, J.C., 2001. Breaking Oswald'srule. Chemie Erde-Geochemie, 61 : 224-235.

De la Rocha, L., DePaolo, D.J., 2000. Isotopic evidence for variations in the marine calcium cycle over the Cenozoic. Science, 289(5482): 1176-1178.

De Leeuw, N.H., Parker, S.C., 2001. Surface-water interaction in the dolomite problem. Physical Chemistry Chemical Physics, 12: 3217-3221.

De Tommaso, D., De Leeuw, N.H., 2008. The onset of calcium carbonate nucleation: A density functional theory molecular dynamics and hybrid microsolvation/continumn study. Journal of Physical Chemistry B, 112: 6965-6975.

De Tommaso, D., De Leeuw, N.H., 2010. The structure and dynamics of the hydrated magnesium ion and of the solvated magnesium carbonates: Insights from first principle calculations. Physical Chemistry Chemical Physics, 12: 894-901.

DePaolo, D.J., 2004. Calcium isotopic variations produced by biological, kinetic, radiogenic and nucleosynthetic processes. Reviews in Mineralogy and Geochemistry, 55(1): 255-288.

DePaolo, D.J., 2011. Surface kinetic model for isotopic and trace element fractionation during precipitation of calcite from aqueous solutions. Geochimica et Cosmochimica Acta, 75(4): 1039-1056.

Fantle, M.S., 2010. Evaluating the Ca isotope proxy. American Journal of Science, 310(3): 194-230.

Fantle, M.S., DePaolo, D.J., 2005. Variations in the marine Ca cycle over the past 20 million years. Earth and Planetary Science Letters, 237(1–2): 102-117.

Fantle, M.S., Higgins, J., 2014. The effects of diagenesis and dolomitization on Ca and Mg isotopes in marine platform carbonates: Implications for the geochemical cycles of Ca and Mg. Geochimica et Cosmochimica Acta, 142: 458-481.

Galy, A., Bar-Matthews, M., Halicz, L., O'Nions, R.K., 2002. Mg isotopic composition of carbonate: insight from speleothem formation. Earth and Planetary Science Letters, 201(1): 105-115.

Galy, A. Yoffe, O.Janney, P.E., Williams, R.W., Cloquet, O., Ludwik A., Wadhwa, M., Hutcheon, I.D., Ramon, E. Carignan, J., 2003. Magnesium isotope heterogeneity of the isotopic standard SRM980 and new reference materials for magnesium-isotope-ratio measurements. Journal of Analytical Atomic Spectrometry, 18(11): 1352-1356.

Gautelier, M., Oelkers, E.H., Schott, J., 1999. An experimental study of dolomite dissolution rates as a function of pH from −0.5 to 5 and temperature from 25 to 80 °C. Chemical Geology, 157(1–2): 13-26.

Gautelier, M., Schott, J., Oelkers, E.H., 2007. An experimental study of dolomite dissolution rates at 80 °C as a function of chemical affinity and solution composition. Chemical Geology, 242(3–4): 509-517.

Gautier, Q., Bénézeth, P., Mavromatis, V. Schott, J., 2014. Hydromagnesite solubility and growth kinetics in aqueous solution from 25 to 75 °C. Geochimica et Cosmochimica Acta, 138:1-20.

Gautier, Q., Bénézeth, P., Schott, J., 2016. Magnesite growth inhibition by organic ligands: An experimental study at 100, 120 and 146 °C. Geochimica et Cosmochimica Acta, 181:101-125.

Gautier, Q., Berninger, U-N., Schott, J., Jordan, G., 2015. Influence of organic ligands on magnesite growth: A hydrothermal atomic force microscopy study. Geochimica et Cosmochimica Acta, 155: 68-85.

Geske, A., Goldstein, R.H., Mavromatis, V., Richter, D.K., Buhl, D., Kluge, T., John, C.M., Immenhauser, A., 2015. The magnesium isotope (δ^{26}Mg) signature of dolomites. Geochimica et Cosmochimica Acta, 149: 131-151.

Gussone, N., Eisenhauer, A., Heuser, A., Dietzel, M., Bock, B., Spero, H.J., Lea, D.W., Bijma, J., Nagler, T.F., 2003. Model for kinetic effects on calcium isotope fractionation (Δ ^{44}Ca) in inorganic aragonite and cultured planktonic foraminifera. Geochimica Et Cosmochimica Acta, 67(7): 1375-1382.

Gussone, N., Bohm, F., Eisenhauer, A., Dietzel, M., Heuser, A., Teichert, B.M.A., Reitner, J., Worheide, G., Dullo, W.C., 2005. Calcium isotope fractionation in calcite and aragonite. Geochimica et Cosmochimica Acta, 69(18): 4485-4494.

Gussone, N., Nehrke, G., Teichert, B.M.A., 2011. Calcium isotope fractionation in ikaite and vaterite. Chemical Geology, 285(1–4): 194-202.

Halicz, L., Galy, A., S. Belshaw, N., O'Nions, K., 1999. High-precision measurement of calcium isotopes in carbonates and related materials by multiple collector inductively coupled plasma mass spectrometry (MC-ICP-MS). Journal of Analytical Atomic Spectrometry, 14(12): 1835-1838.

Hamm, L.M., Wallace, A.F., Dove, P.M., 2010. Molecular dynamics of ion hydration in the presence of small carboxylated molecules for calcification. Journal of Physical Chemistry B 114: 10488-10495.

Hauser, A., Eisenhauer, A., Bohm. F., Walmann, K., Gussone, N., Pearson, P.N., Nagler, T.F., Dullo, W.C., 2005. Calcium isotope (delta $^{44/40}$Ca) variations of Neogene planktonic foraminfera. Paleoceanography 20(2): PA2013.

Higgins, J.A., Schrag, D.P., 2010. Constraining magnesium cycling in marine sediments using magnesium isotopes. Geochimica et Cosmochimica Acta, 74(17): 5039-5053.

Higgins, S.R., Hu, X., 2005. Self-limiting growth on dolomite: Experimental observations with in situ atomic force microscopy. Geochimica et Cosmochimica Acta, 69(8): 2085-2094.

Hippler, D., Buhl, D., Witbaard, R., Richter, D. K., Immenhauser, A., 2009. Towards a better understanding of magnesium-isotope ratios from marine skeletal carbonates. Geochimica et Cosmochimica Acta, 73(20): 6134-6146.

Hippler, D., Schmitt, A-D., Gussone, N., Heuser, A., Stille, P., Eisenhauer, A., Nägler,T. F., 2003. Calcium isotopic composition of various reference materials and seawater. Geostandards Newsletter, 27(1): 13–19.

Holland, H.D., 2005. Sea level, sediments, and the composition of seawater. American Journal of Science, 305, 220-239.

Holmden, C., 2009. Ca isotope study of Ordovician dolomite, limestone, and anhydrite in the Williston Basin: Implications for subsurface dolomitization and local Ca cycling. Chemical Geology, 268(3–4): 180-188.

Hong, M., Xu, J., Teng, H.H., 2016. Evolution of calcite growth morphology in the presence of magnesium: Implications for the dolomite problem. Geochimica et Cosmochimica Acta, 172: 55-64.

Ilina, S. M., Viers, J., Lapitsky, S. A., Mialle, S., Mavromatis, V., Chmeleff, J., Brunet, P., Alekhin, Y. V., Isnard, H., Pokrovsky, O. S., 2013. Stable (Cu, Mg) and radiogenic (Sr, Nd) isotope fractionation in colloids of boreal organic-rich waters. Chemical Geology, 342: 63-75.

Ijkeda, T., Boero, M., Terakura, K., 2007. Hydration properties of magnesium and calcium ions constrained from first principles molecular dynamics. Journal of Chemical Physics, 127: 074503.

Immenhauser, A., Buhl, D., Richter, D., Niedermayr, A., Reichelmann, D., Dietzel, M., Schulte, U., 2010. Magnesium-isotope fractionation during low-Mg calcite precipitation in a limestone cave – Field study and experiments. Geochimica et Cosmochimica Acta, 74(15): 4346-4364.

Jacobson, A.D., Zhang, Z., Lundstrom, C., Huang, F., 2010. Behavior of Mg isotopes during dedolomitization in the Madison Aquifer, South Dakota. Earth and Planetary Science Letters, 297(3): 446-452.

Kasemann, S.A., Pogge von Strandmann, P.A.E., Prave, A.R., Fallick, A.E., Elliott, T., Hoffmann, K-H., 2014. Continental weathering following a Cryogenian glaciation: Evidence from calcium and magnesium isotopes. Earth and Planetary Science Letters, 396: 66-77.

Katz, A. Matthews, A., 1977. The dolomatization of $CaCO_3$: An experimental study at 252-295 ^{o}C. Geochimica et Cosmochimica Acta, 41: 297-304.

Kessels, L.A., Sibley, D.F., Nordeng, S.H., 2000. Nanotopography of synthetic and natural dolomite crystals. Sedimentology, 47(1): 173-186.

Land, L.S. 1980. The isotopic and trace element geochemistry of dolomite: The state of the art. In D.H. Zenger, J.B. Dunham and R.L. Ethington (Eds.), Concepts and Models of Dolomitisation. Society of Economic Paleontologists and Mineralogists, Special Publication no. 28, p. 87-110.

Land, L.S., 1998. Failure to precipitate dolomite at 25 °C from dilute solution despite 1000-fold oversaturation after 32 Years. Aquatic Geochemistry, 4(3): 361-368.

Lerbermann, O., 1967. Synthesis of dolomite. Nature, 213: 241-245.

Lemarchand, D., Wasserburg, G.J., Papanastassiou, D.A., 2004. Rate-controlled calcium isotope fractionation in synthetic calcite. Geochimica et Cosmochimica Acta, 68(22): 4665-4678.

Li, W., Beard, B.L., Li, C., Johnson, C.M., 2014. Magnesium isotope fractionation between brucite [$Mg(OH)_2$] and Mg aqueous species: Implications for silicate weathering and biogeochemical processes. Earth and Planetary Science Letters, 394: 82-93.

Li, W., Beard, B.L., Li, C., Xu, H., Johnson, C.M., 2015. Experimental calibration of Mg isotope fractionation between dolomite and aqueous solution and its geological implications. Geochimica et Cosmochimica Acta, 157: 164-181.

Li, W., Chakraborty, S., Beard, B.L., Romanek, C.S., Johnson, C.M., 2012. Magnesium isotope fractionation during precipitation of inorganic calcite under laboratory conditions. Earth and Planetary Science Letters, 333: 304-316.

Libbermann, O., 1967. Synthesis of dolomite. Nature, 213: 241-245.

Linder, M., Saldi, G.S., Jordan, G., Schott, J., 2017. On the effect of aqueous barium on magnesite growth – A new route for the precipitation of the ordered anhydrous Mg-beating double carbonate norsethite. Chemical Geology, 460, 93-105.

Lippmann, F., 1973. Sedimentary Carbonate Minerals. Springer-Verlag, Berlin, 228 p.

Liu, Z., Rimstidt, J.D., Zhang, Y., Yuan, H., Zhu, C., 2016. A stable isotope doping method to test the range of applicability of detailed balance. Geochemical Perspectives Letters, 2(0): 78-86.

Lund, K., Fogler, H.S., McCune, C.C., 1973. Acidization—I. The dissolution of dolomite in hydrochloric acid. Chemical Engineering Science, 28(3): 691-IN1.

Maher, K., Johnson, N. C., Jackson, A., Lammers, L. N., Torchinsky, A. B., Weaver, K. L., Bird, D. K., Brown Jr, G. E., 2016. A spatially resolved surface kinetic model for forsterite dissolution. Geochimica et Cosmochimica Acta, 174: 313-334.

Marriott, C.S., Henderson, G.M., Belshaw, N.S., Tudhope, A.W., 2004. Temperature dependence of δ^7Li, δ^{44}Ca and Li/Ca during growth of calcium carbonate. Earth and Planetary Science Letters, 222(2): 615-624.

Mavromatis, V., Gautier, Q., Bosc, O., Schott, J., 2013. Kinetics of Mg partition and Mg stable isotope fractionation during its incorporation in calcite. Geochimica et Cosmochimica Acta, 114: 188-203.

Mavromatis, V., Meister, P., Oelkers, E.H., 2014a. Using stable Mg isotopes to distinguish dolomite formation mechanisms: A case study from the Peru Margin. Chemical Geology, 385: 84-91.

Mavromatis, V., Pearce, C.R., Shirokova, L.S., Bundeleva, I.A., Pokrovsky, O.S., Benezeth, P., Oelkers, E.H., 2012. Magnesium isotope fractionation during hydrous magnesium carbonate precipitation with and without cyanobacteria. Geochimica et Cosmochimica Acta, 76: 161-174.

Mavromatis, V., Prokushkin, A.S., Pokrovsky, O.S., Viers, J., Korets, M.A., 2014b. Magnesium isotopes in permafrost-dominated Central Siberian larch forest watersheds. Geochimica et Cosmochimica Acta, 147: 76-89.

McKinney, C.R., McCrea, J.M., Epstein, S., Allen, H.A., Urey, H.C., 1950. Improvements in mass spectrometers for the measurement of small differences in isotope abundance ratios. Review of Scientific Instruments, 21(8): 724-730.

Morse, J.W., Arvidson, R.S., 2002. The dissolution kinetics of major sedimentary carbonate minerals. Earth-Science Reviews, 58(1–2): 51-84.

Nielsen, L.C., Druhan, J.L., Yang, W., Brown, S.T., DePaolo, D.J., 2012. Calcium Isotopes as Tracers of Biogeochemical Processes. In: Baskaran, M. (Ed.), Handbook of Environmental Isotope Geochemistry: Vol I. Springer Berlin Heidelberg, Berlin, Heidelberg, pp. 105-124.

Oelkers, E.H., 2001. General kinetic description of multioxide silicate mineral and glass dissolution. Geochimica et Cosmochimica Acta, 65(21): 3703-3719.

Oelkers, E.H., Golubev, S.V.,Chairat,C., Pokrovsky, O.S., Schott, J., 2009. The surface chemistry of multi-oxide silicates. Geochimica et Cosmochimica Acta 173, 4617-4634.

Parkhurst, D.L., Appelo, C.A.J., 1999. User's guide to PHREEQC (Version 2): A computer program for speciation, batch-reaction, one-dimensional transport, and inverse geochemical calculations.

Pearce, C.R., Saldi, G.D., Schott, J., Oelkers, E.H., 2012. Isotopic fractionation during congruent dissolution, precipitation and at equilibrium: Evidence from Mg isotopes. Geochimica et Cosmochimica Acta, 92: 170-183.

Pimentel, C., Pina, C.M., 2014. The formation of the dolomite-analogue norsethite : Reaction path and ordering. Geochimica et Cosmochimica Acta, 142: 217-223.

Pimentel, C., Pina, C.M., 2016. Reaction pathways towards the formation of dolomite-aalogues at ambient conditions. Geochimica et Cosmochimica Acta, 178: 259-267.

Pinilla, C., Blanchard, M., Balan, E., Natarajan, S. K., Vuilleumier, R., Mauri, F., 2015. Equilibrium magnesium isotope fractionation between aqueous Mg^{2+} and carbonate minerals: Insights from path integral molecular dynamics. Geochimica et Cosmochimica Acta, 163: 126-139.

Pogge von Strandmann, P.A.E., Burton, K. W., James, R. H., van Calsteren, P., Gislason, S. R., Sigfússon, B., 2008. The influence of weathering processes on riverine magnesium isotopes in a basaltic terrain. Earth and Planetary Science Letters, 276(1–2): 187-197.

Pogge von Strandmann, P.A.E., Opfergelt, S., Lai, Y.-J., Sigfusson, B., Gislason, S.R., Burtin, K., 2012. Lithium, magnesium and silicon isotope behaviour accompanying weathering in a basaltic soil and pore water profile in Iceland. Earth and Planetary Science Letters, 339: 11-23.

Pogge von Strandmann, P.A.E., Forshaw, J., Schmidt, D.N., 2014. Modern and Cenozoic record of seawater magnesium form foraminiferal Mg isotopes Biogeosciences, 11 (2014): 5155–5168

Pokrovsky, B. G., Mavromatis, V., Pokrovsky, O. S., 2011. Co-variation of Mg and C isotopes in late Precambrian carbonates of the Siberian Platform: A new tool for tracing the change in weathering regime? Chemical Geology, 290(1–2): 67-74.

Pokrovsky, O.S., Golubev, S.V., Schott, J., 2005. Dissolution kinetics of calcite, dolomite and magnesite at 25 °C and 0 to 50 atm pCO_2. Chemical Geology, 217(3–4): 239-255.

Pokrovsky, O.S., Golubev, S.V., Schott, J., Castillo, A., 2009. Calcite, dolomite and magnesite dissolution kinetics in aqueous solutions at acid to circumneutral pH, 25 to 150 °C and 1 to 55 atm pCO_2: New constraints on CO_2 sequestration in sedimentary basins. Chemical Geology, 265(1–2): 20-32.

Pokrovsky, O.S., Schott, J., 1999. Processes at the magnesium-bearing carbonates/solution interface. II. kinetics and mechanism of magnesite dissolution. Geochimica et Cosmochimica Acta, 63(6): 881-897.

Pokrovsky, O.S., Schott, J., 2001. Kinetics and mechanism of dolomite dissolution in neutral to alkaline solutions revisited. American Journal of Science, 301(7): 597-626.

Pokrovsky, O.S., Schott, J., Thomas, F., 1999a. Dolomite surface speciation and reactivity in aquatic systems. Geochimica et Cosmochimica Acta, 63(19–20): 3133-3143.

Pokrovsky, O.S., Schott, J., Thomas, F., 1999b. Processes at the magnesium-bearing carbonates/solution interface. I. A surface speciation model for magnesite. Geochimica et Cosmochimica Acta, 63(6): 863-880.

Putnis, C.V., Ruiz-Agudo, E., Hövelmann, J., 2014. Coupled fluctuations in element release during dolomite dissolution. Mineralogical Magazine, 78(6): 1355-1362.

Reynard, L.M., Henderson, G.M., Hedges, R.E.M., 2010. Calcium isotope ratios in animal and human bone. Geochimica et Cosmochimica Acta, 74(13): 3735-3750.

Reynard, L.M., Day, C.C., Henderson, G.M., 2011. Large fractionation of calcium isotopes during cave-analogue calcium carbonate growth. Geochimica et Cosmochimica Acta., 75 :3726-3740.

Richter, F. M., Mendybaev, R. A., Christensen, J. N., Hutcheon, I. D., Williams, R. W., Sturchio, N. C., Beloso Jr., A. D., 2006. Kinetic isotopic fractionation during diffusion of ionic species in water. Geochimica et Cosmochimica Acta 70(2): 277-289.

Roberts, J.A., Kenward, P.A., Fowle, D.A., Goldstein, R.H., Gonzalez, L.A., Moore, D.S., 2013. Surface chemistry allows for abiotic precipitation of dolomite at low temperature. Proceeding of the National Academy of Sciences, 110: 14540-14545.

Rodriguez-Blanco, J.D., Shaw, S., Benning, L.G., 2015. A route for the direct crystallization of dolomite. American Mineralogist, 100(5-6): 1172-1181.

Rollion-Bard, C., Saulnier, S., Vigier, N., Schumacher, A., Chaussidon, M., Lécuyer, C., 2016. Variability in magnesium, carbon and oxygen isotope compositions of brachiopod shells: Implications for paleoceanographic studies. Chemical Geology, 423: 49-60.

Rustad, J.R., Casey, H., Qing-Zhu Y., Dixon, D.A., 2010. Isotopic fractionation of Mg^{2+}(aq), Ca^{2+}(aq), and Fe^{2+}(aq) with carbonate minerals. Geochimica et Cosmochimica Acta, 74(22): 6301-6323.

Saldi, G.D., Jordan, G., Schott, J., Oelkers, E.H., 2009. Magnesite growth rates as a function of temperature and saturation state. Geochimica et Cosmochimica Acta, 73(19): 5646-5657.

Saldi, G.D., Schott, J., Pokrovsky, O.S., Gautier, Q., Oelkers, E.H., 2012. An experimental study of magnesite precipitation rates at neutral to alkaline conditions and 100–200 °C as a function of pH, aqueous solution composition and chemical affinity. Geochimica et Cosmochimica Acta, 83: 93-109.

Saulnier, S., Rollion-Bard, C., Vigier, N., Chaussidon, M., 2012. Mg isotope fractionation during calcite precipitation: An experimental study. Geochimica et Cosmochimica Acta, 91: 75-91.

Schauble, E.A., 2011. First-principles estimates of equilibrium magnesium isotope fractionation in silicate, oxide, carbonate and hexaaquamagnesium (2+) crystals. Geochimica et Cosmochimica Acta, 75(3): 844-869.

Schott, J., Oelkers, E.H., 1995. Dissolution and crystallization rates of silicate minerals as a function of chemical affinity. Pure and applied chemistry, 67(6): 903-910.

Schott, J., Pokrovsky, O.S., Oelkers, E.H., 2009. The link between mineral dissolution/precipitation kinetics and solution chemistry. Reviews in Mineralogy and geochemistry, 70(1): 207-258.

Schott, J., Oelkers, E.H., Benexeth, P., Godderis, Y., Francois, L., 2012. Can accurate rate laws be created to describe chemical weathering? Comptes Rendus Geoscience, 344(11), 568-585.

Schott, J., Mavromatis, V., Fujii, T., Pearce, C.R., Oelkers, E.H., 2016. The control of carbonate mineral Mg isotope composition by aqueous speciation: Theoretical and experimental modeling. Chemical Geology, DOI: 10.1016/j.chemgeo.2016.03.011

Shirokova, L.S., Mavromatis, V., Bundeleva, I. A., Pokrovsky O.S., Bénézeth, P., Gérard, E., Pearce, C. R., Oelkers, E. H., 2013. Using Mg Isotopes to Trace Cyanobacterially Mediated Magnesium Carbonate Precipitation in Alkaline Lakes. Aquatic Geochemistry, 19(1): 1-24

Sibley, D.F., Dedoes, R.E., Bartlett, T.R., 1987. The kinetics of dolomitizaion. Geology, 15, 1112-1114.

Sime, N.G., deLa Rocha, C.L., Tipper, E.T., Tripati, A., Galy, A., Bickle, M.J., 2007. Interpreting the Ca isotope record of marine biogenic carbonates. Geochimica et Cosmochimica Acta, 71(16): 3979-3989.

Skulan, J., DePaolo, D.J., Owens, T.L., 1997. Biological control of calcium isotopic abundances in the global calcium cycle. Geochimica et Cosmochimica Acta, 61(12): 2505-2510.

Slaughter, M, Hill, R.J., 1991. The influence of organic matter in organogenic dolomitization. Journal of Sedimentary Research, 61:296-303.

Tang, J., Dietzel, M., Böhm, F., Köhler, S.J., Eisenhauer, A., 2008a. Sr^{2+}/Ca^{2+} and $^{44}Ca/^{40}Ca$ fractionation during inorganic calcite formation: II. Ca isotopes. Geochimica et Cosmochimica Acta, 72(15): 3733-3745.

Tang, J., Köhler, S.J., Dietzel, M., 2008b. Sr^{2+}/Ca^{2+} and $^{44}Ca/^{40}Ca$ fractionation during inorganic calcite formation: I. Sr incorporation. Geochimica et Cosmochimica Acta, 72(15): 3718-3732.

Urey, H.C., 1948. Oxygen isotopes in nature and in the laboratory. Science, 108(2810): 489-496.

Van Cappellen, P., Charlet, L., Stumm, W., Wersin, P., 1993. A surface complexation model of the carbonate mineral-aqueous solution interface. Geochimica et Cosmochimica Acta, 57(15): 3505-3518.

Vasconcelos, C., McKenzie, J.A., Warthmann, R., Bernasconi, S.M., 2005. Calibration of the $\delta^{18}O$ paleothermometer for dolomite precipitated in microbial cultures and natural environments. Geology, 33(4).

Wang, X., Chou, I.-M., Hu, W., Yaun, S., Lui, H., Wan, Y., Wang, X., 2016, Kinetic inhibition of dolomite precipitation: Insights from Raman spectroscopy of Mg^{2+}-SO_4^{2-} ion paring in $MgSO_4/MgCl_2$/NaCl solutions at temperatures of 25 to 200 ^oC. Chemical Geology, 435: 10-21.

Wollast, R., 1990. Rate and mechanism of dissolution of carbonates in the system $CaCO_3$-$MgCO_3$. In: Aquatic Chemical Kinetics: Reaction Rates of Processes in Natural Waters. Environmental Science and Technology Series. John Wiley & Sons, New York. 1990. p 431-445.

Wombacher, F., Eisenhauer, A., Heuser, A., Weyer, S., 2009. Separation of Mg, Ca and Fe from geological reference materials for stable isotope ratio analyses by MC-ICP-MS and double spike TIMS. Journal of Analytical Atomic Spectrometry, 24, 627-636.

Wombacher, F., Eisenhauer, A., Böhm, F., Gussone, N., Regenberg, M., Dullo, W. Chr., Rüggeberg, A., 2011. Magnesium stable isotope fractionation in marine biogenic calcite and aragonite. Geochimica et Cosmochimica Acta, 75(19): 5797-5818.

Yang, Y., Sahai, N., Romanek, C.S., Chakraborty, S. 2012. A computational study of Mg^{2+} dehydration in aqueous solution in the presence of HS^- and other monovalent anions – Insights to dolomite formation. Geochimica et Cosmochimica Acta, 88, 77-87.

Young, E.D., Galy, A., 2004. The isotope geochemistry and cosmochemistry of magnesium. Reviews in Mineralogy and Geochemistry, 55: 197-230.

Zhang, F.F., Xu, H.F., Konishi, H., Roden, E.E., 2010. A relationship between d(104) value and composition in the calcite-disordered dolomite solid solution serties. American Mineralogist, 95 : 1650, 1656.

Zhang, R., Hu, S., Zhang, X., Yu, W., 2007. Dissolution kinetics of dolomite in water at elevated temperatures. Aquatic Geochemistry, 13(4): 309-338.

Zhu, P., Macdougall, J.D., 1998. Calcium isotopes in the marine environment and the oceanic calcium cycle. Geochimica et Cosmochimica Acta, 62(10): 1691-1698.

Fig. 1. Representative Scanning Electron Microscope (SEM) photographs of the dolomite used in this study. (A) Unreacted seeds, (B), (C) and (D) aspect of the dolomite after the dissolution experiments at 51, 75, and 126 °C respectively.

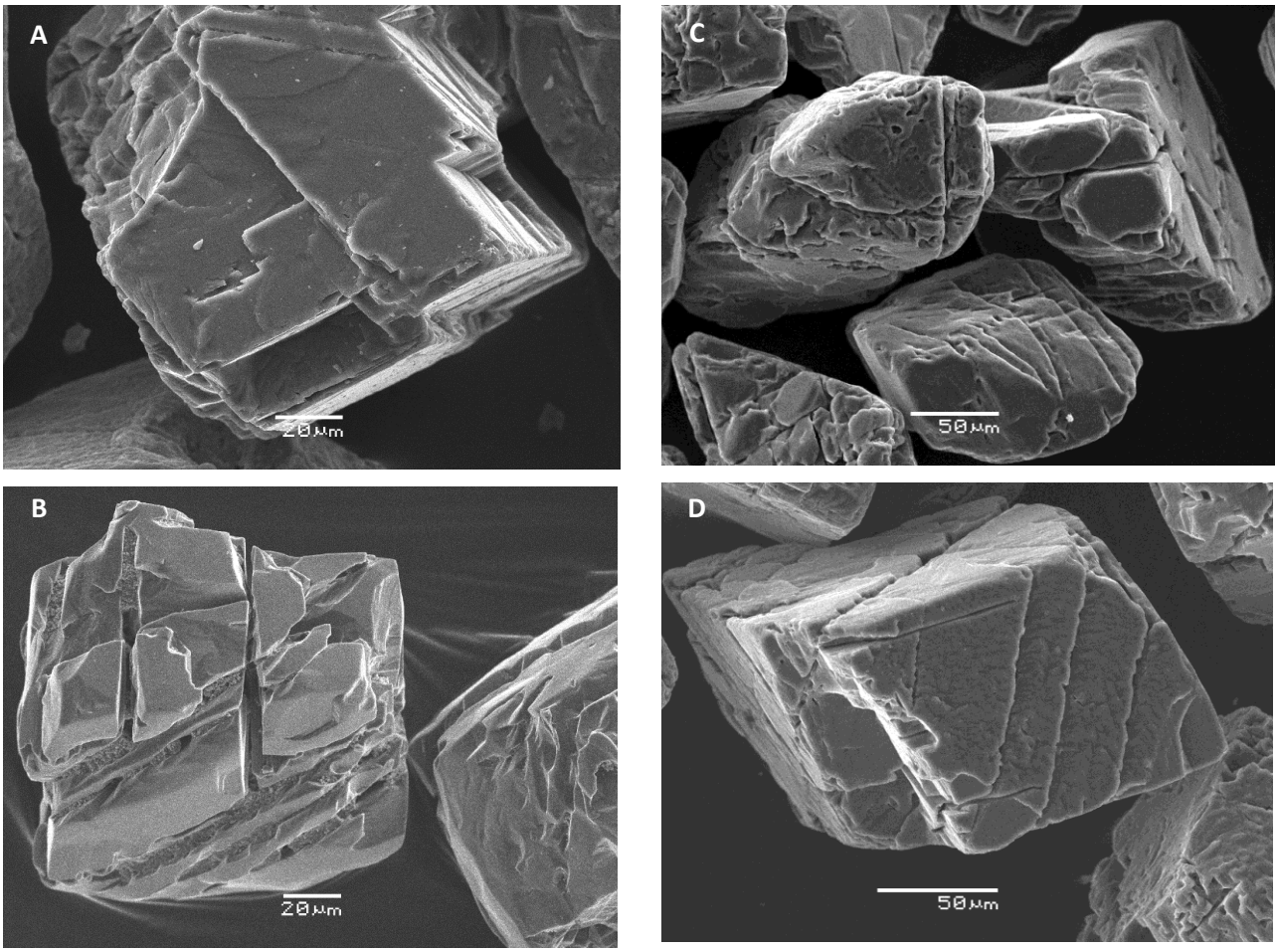

Fig. 2. (A) Temporal evolution of fluid calcium and magnesium concentrations, $C_{Ca,fluid}$ (open symbols) and $C_{Mg,fluid}$ (black symbols). Analytical uncertainties in concentration and error bars are $\pm$3%. (B) pH evolution during the experiments. (C) Temporal variation of logarithm of reactive fluid saturation index with respect to dolomite (log Ω).

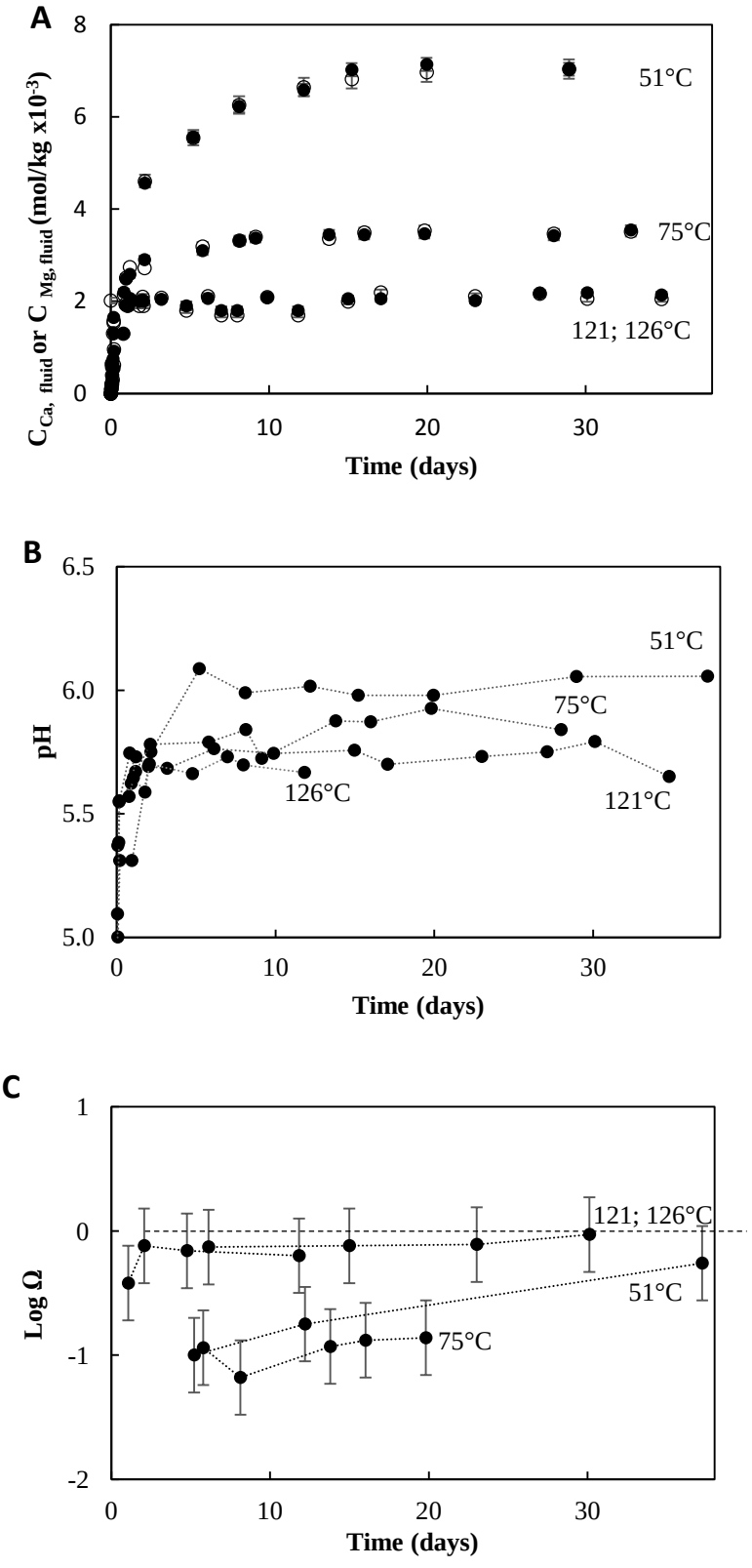

Fig. 3. Temporal evolution of the reactive fluid Ca and Mg concentration, $C_{Ca,fluid}$ and $C_{Mg,fluid}$ (black circles), and $\Delta^{26/24}Ca_{fluid\text{-}solid}$ or $\Delta^{26/24}Mg_{fluid\text{-}solid}$ (x symbols) respectively during the experiments at 51, 75, 121, and 126°C. The dashed line and its shading corresponds to the composition of the initial solid and its associated 2σ uncertainty.

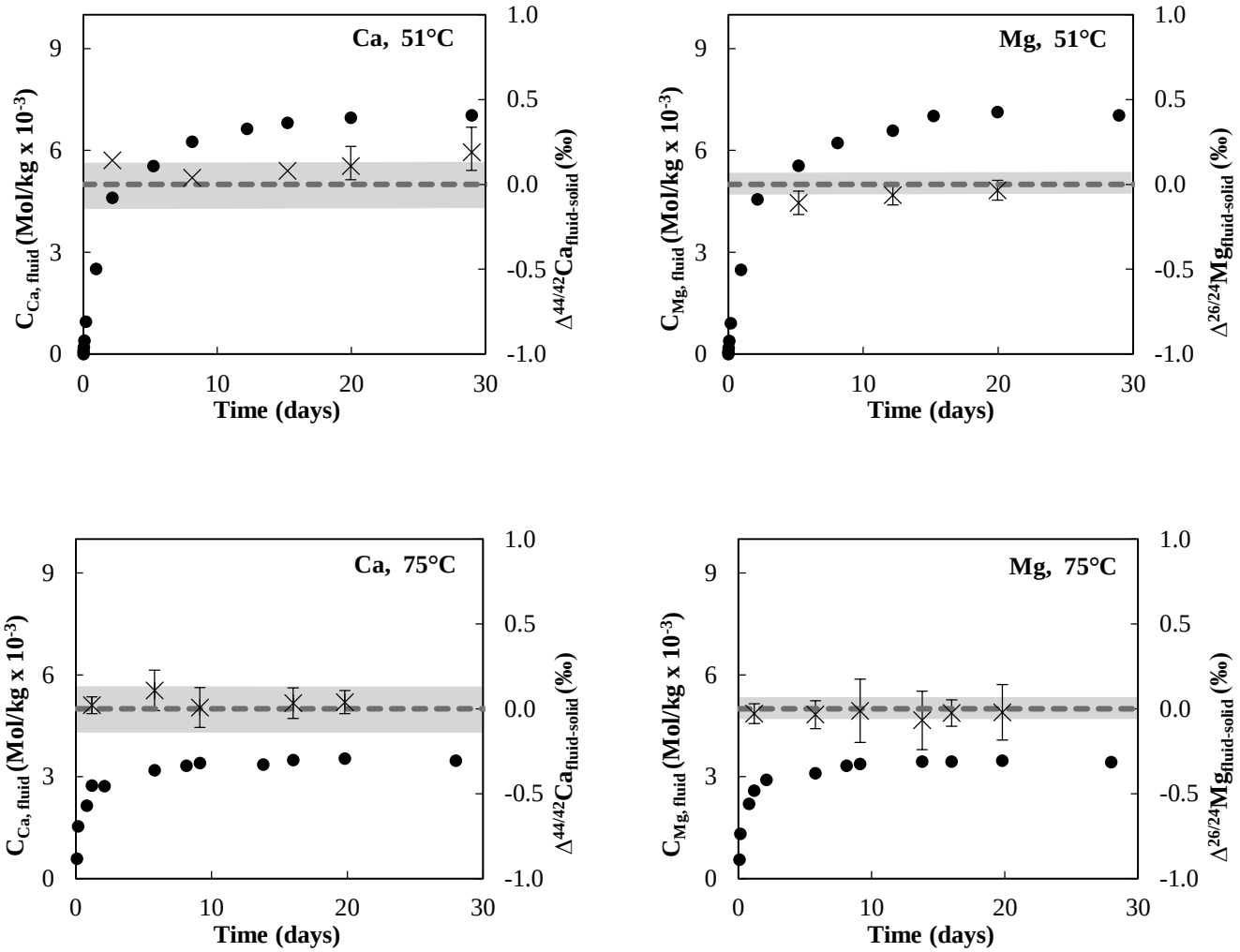

Fig. 3 (Continued)

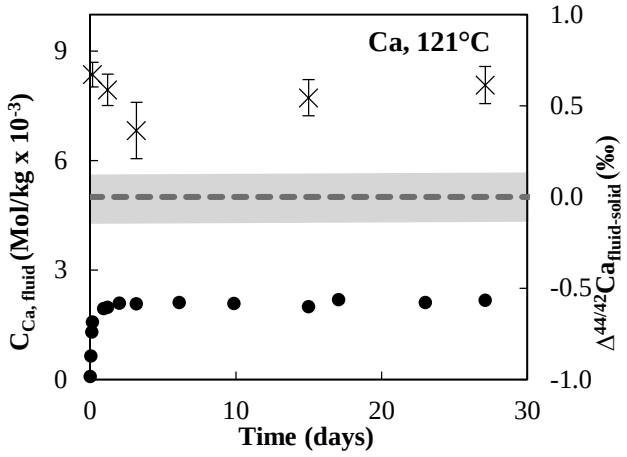

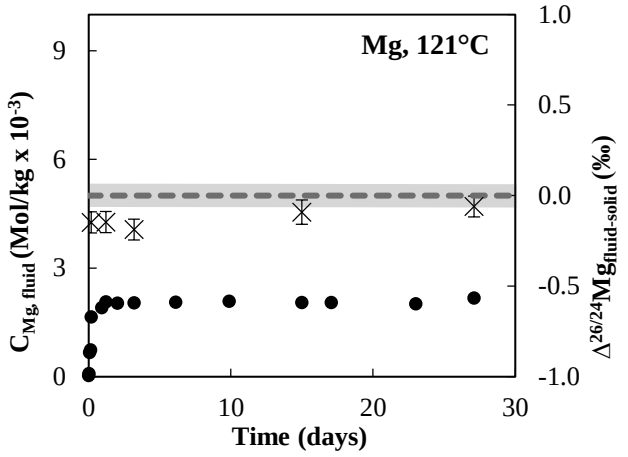

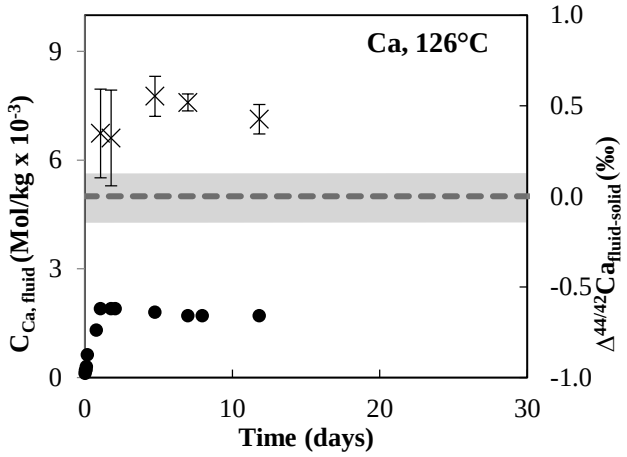

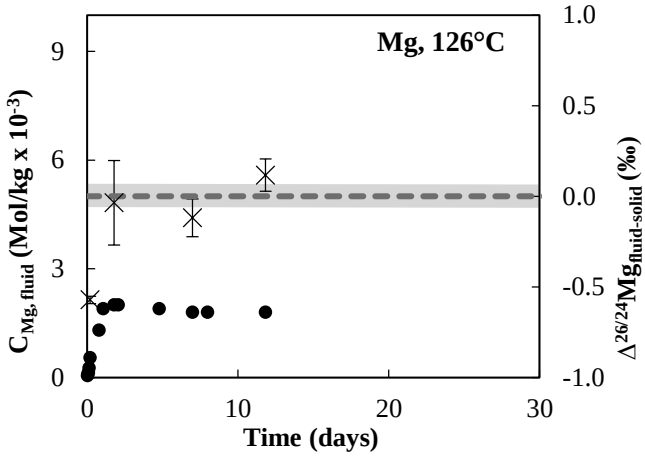

Fig. 4. Schematic illustration showing the potential isotope fractionation mechanism in dolomite as a function of temperature. At temperatures lower than 100°C dissolution consists of only the forward dissolution step for both Mg and Ca in the absence of back reaction. Forward dissolution proceeds without isotope fractionation. At higher temperatures (121 and 126 ^{o}C) and close to equilibrium conditions the backward reaction becomes important Ca but not for Mg. This backward reaction can fractionate Ca isotopes as it reincorporates this metal into the dolomite structure.

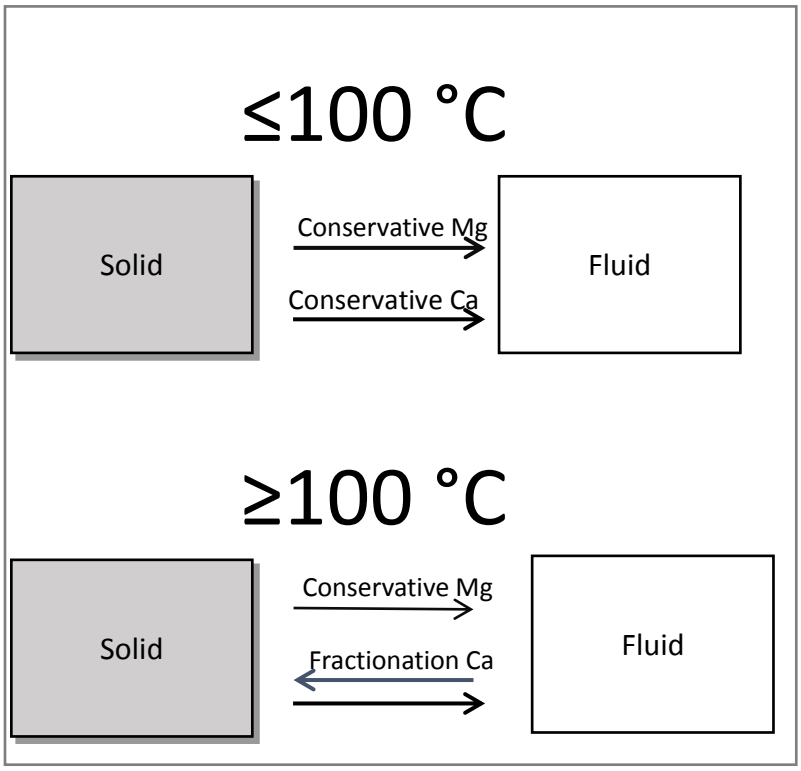

Table 1

Chemical composition of the initial Sainte Colombe dolomite seeds before the experiments described in this study.

Oxide	Mol % oxide
CaO	34.35
MgO	22.72
FeO	0.0122
MnO	0.0075
TiO_2	0.0092
Cr_2O_3	0.0026
Al_2O_3	0.0033
SiO_2	0.0122
Na_2O	0.0037
K_2O	0.0017
calculated CO_2	42.89
chem. formula	$Ca_{1.04}Mg_{0.96}(CO_3)_2$

Table 2

Summary of initial experimental conditions used in the dolomite dissolution experiments. pCO_2 was 5 bars. The stirring rate was 200 rpm and the surface area of the original powder was 0.717m^2/g.

Experiment	Av. Temperature (°C)	pH	initial dolomite mass (g)	Initial fluid mass (g)
Dol51	51.28	6.1	1.068	451
Dol75	74.96	5.9	1.012	442
Dol121	120.73	5.9	1.014	434
Dol126	126.5	5.7	1.074	462

Table 3

Results from the dolomite dissolution experiments at 121 and 126°C. $\delta^{44/42}Ca_{solid}$ (‰) and $\delta^{26/24}Mg_{solid}$ (‰) of the solid were obtained from the corresponding fluid isotopic compositions using mass balance calculations.

Sample	Time (days)	Temp (°C)	pH sample	Ca (mol/kg x10^{-3})	Mg (mol/kg x10^{-3})	Solid dissolved %	Ca/Mg	Alk	$\delta^{26/24}$ Mg (‰)	2 s.d.	$\Delta^{26/24}$ Mg solid-fluid	$\delta^{44/42}$ Ca (‰)	2 s.d.	$\Delta^{44/42}$ Ca solid-fluid
Inlet solid for experiments at 51, 71 and 121 °C							1.00		-1.62	0.058		0.60	0.139	
51.1	0.00	58.3	3.72	0.00	0.00	0	0.00							
51.2	0.01	60.1	4.61	0.09	0.08	1	1.13							
51.3	0.03	53.7	4.88	0.20	0.19	2	1.05							
51.4	0.07	51.4	5.00	0.40	0.39	3	1.03							
51.5	0.20	49.9	5.31	0.96	0.92	7	1.04	0.004						
51.6	0.95	53.1	6.99	2.51	2.48	20	1.01							
51.7	2.16	49.7	7.27	4.61	4.56	36	1.01					0.74	0.225	-0.142
51.8	5.21	50.2	6.09	5.55	5.56	43	1.00	0.021	-1.73	0.068	0.109			
51.9	8.11	52.4	5.99	6.26	6.22	49	1.01					0.64	0.142	-0.040
51.10	12.20	50	6.02	6.64	6.58	52	1.01	0.022	-1.68	0.039	0.062			
51.11	15.22	51.9	5.98	6.82	7.02	53	0.97					0.68	0.115	-0.080
51.12	19.96	50.6	5.98	6.97	7.14	54	0.98		-1.65	0.031	0.034	0.70	0.146	-0.108
51.14	28.96	51.5	6.06	7.03	7.03	55	1.00					0.78	0.099	-0.190
51.15	37.22	52.2	6.06	6.69	6.62	52	1.01	0.030						
51.16	47.98	50.7	6.21	6.67	6.59	52	1.01							
75.1	0.08	75.1	5.37	0.58	0.55	5	1.05							
75.2	0.17	75	5.55	1.53	1.31	12	1.17							
75.3	0.82	75	5.75	2.15	2.20	17	0.98							
75.4	1.19	75	5.67	2.74	2.59	21	1.06	0.006	-1.65	0.047	0.028	0.62	0.049	-0.021
75.5	2.12	74.9	5.78	2.72	2.90	21	0.94	0.005						
75.6	5.80	75	5.79	3.18	3.10	25	1.03	0.012	-1.65	0.083	0.035	0.70	0.119	-0.108
75.7	8.13	74.9	5.84	3.32	3.32	26	1.00	0.010						
75.8	9.14	74.9	5.72	3.40	3.37	26	1.01	0.008	-1.63	0.187	0.012	0.60	0.118	-0.007
75.9	13.80	75.2	5.88	3.35	3.45	26	0.97	0.011	-1.69	0.172	0.068	0.57	0.096	0.030
75.10	16.01	75	5.87	3.49	3.45	27	1.01	0.012	-1.64	0.078	0.025	0.63	0.090	-0.033
75.11	19.82	74.9	5.93	3.53	3.47	27	1.02	0.012	-1.64	0.164	0.021	0.64	0.068	-0.039
75.12	27.99	75	5.84	3.47	3.43	27	1.01							

Table 3 (Continued)

Sample	Time (days)	Temp (°C)	pH $_{sample}$	Ca (mol/kg x10^{-3})	Mg (mol/kg x10^{-3})	Solid $_{dissolved}$ %	Ca/Mg	Alk	$\delta^{26/24}$ Mg (‰)	2 s.d.	$\Delta^{26/24}$Mg $_{solid-fluid}$	$\delta^{44/42}$ Ca (‰)	2 s.d.	$\Delta^{44/42}$ Ca $_{solid-fluid}$
121.2	0.00	32.6	2.10	0.25	0.04	1	6.25							
121.3	0.01	61.8	3.11	0.08	0.09	5	0.89							
121.4	0.06	100.6	5.10	0.64	0.67	10	0.96							
121.5	0.13	124.1	5.38	1.31	0.75	12	1.75							
121.6	0.17	117.6	5.55	1.57	1.65	15	0.95		-1.77	0.023	0.148	1.27	0.068	-0.670
121.7	0.93	115.7	5.62	1.94	1.91	15	1.02							
121.8	1.21	120.3	5.73	1.98	2.07	16	0.96		-1.77	0.007	0.146	1.18	0.086	-0.587
121.9	2.01	120.6	5.69	2.09	2.03	16	1.03							
121.10	3.19	121.1	5.68	2.07	2.04	16	1.01		-1.81	0.022	0.187	0.96	0.154	-0.364
121.11	6.13	121.1	5.76	2.11	2.06	16	1.02	0.007						
121.12	9.89	121	5.74	2.09	2.09	15	1.00							
121.13	14.99	121	5.76	2.00	2.05	17	0.98	0.007	-1.71	0.067	0.091	1.14	0.099	-0.544
121.14	17.07	121.5	5.70	2.19	2.05	16	1.07							
121.15	23.02	121.5	5.73	2.11	2.02	17	1.04	0.007						
121.16	27.11	121.6	5.75	2.17	2.18	16	1.00		-1.68	0.012	0.060	1.21	0.101	-0.614
121.17	30.12	121.6	5.79	2.05	2.19	16	0.94	0.007						
121.18	34.81	121.6	5.65	2.05	2.14	16	0.96							
Inlet solid for experiment at 126°C									-1.21	0.110	0.000	0.183	0.045	
126.1	0.031	70.0	6.2	0.11	0.05	0	2.20							
126.2	0.052	85.5	5.92	0.19	0.08	1	2.38							
126.3	0.083	99.0	5.79	0.21	0.14	1	1.50							
126.4	0.119	108.2	5.36	0.30	0.26	2	1.15							
126.5	0.188	113.9	5.18	0.62	0.54	2	1.15	0.002	-1.78	0.020	-0.573			
126.6	0.779	115.7	5.57	1.29	1.28	5	1.00							
126.7	1.067	116.1	5.65	1.99	1.94	9	1.00	0.006				0.53	0.245	0.347
126.8	1.785	130.4	5.59	2.00	2.01	14	0.95		-1.24	0.233	-0.037	0.50	0.264	0.322
126.9	2.065	125.5	5.70	1.90	1.96	14	0.95	0.007						
126.10	4.769	126.8	5.66	1.83	1.89	12	0.95	0.007				0.73	0.111	0.552
126.11	6.983	126.4	5.73	1.70	1.86	12	0.94		-1.33	0.104	-0.119	0.70	0.047	0.518
126.12	7.978	127.0	5.70	1.73	1.84	11	0.94	0.007						
126.13	11.82	127.2	5.67	1.70	1.84	11	0.94	0.006	-1.09	0.090	0.116	0.60	0.081	0.425
Isotopic standards														
CAM-1									-2.67	0.05				
OUMg									-2.76	0.08				
DSM-3									0.00	0.03				
JDo-1									-2.40	0.02		1.06	0.12	
IAPSO												0.46	0.11	